*Optica Applicata, Vol. XIX, No. 4, 1989*

# Influence of the field truncation by the aperture stop of interferometers upon the intensity distribution in the observation field*

R. JÓŹWICKI, J. WÓJCIAK

Institute of Design of Precise and Optical Instruments, Warsaw University of Technology, ul. Karola Chodkiewicza 8, 02–525 Warszawa, Poland.

The influence of a truncation introduced by the aperture stop of an interferometric system is studied theoretically. The cases with the uniform illumination and the Gaussian apodisation are considered. The oscillatory intensity changes in the observation field are found, being, however, negligibly small in the majority of practical cases. The phenomenon may be essential in the multipass interferometry, when a strong truncation is applied. The experimental verification is presented.

## 1. Introduction

In interferometers some main fragments that perform different roles can be distinguished. An optical system forming the wavefront impinging onto the standard and measured elements (e.g., a collimator for the flatness measurement) and a system imaging the fringes on a detector are the most typical ones. As yet the whole interferometric system, because of its complexity, has not been considered simultaneously in the interference theory, The planar or spherical wavefront of the propagating beams is assumed to find the fringe equations [1], the ideal standard and tested surfaces are taken to determine the influence of the wave aberrations [2], the distortion introduced by the imaging systems is also considered separately. Our proposition is to supplement these partial analyses by the study on the influence of the aperture stop upon the intensity distribution in the observation field of the interferometric system.

In interferometers, like in other optical systems, some additional useless beams can be generated. The source of such beams is, for example, the reflection from the opposite sides of both the standard and the tested element. Te useless light beams introduce a noise into the observation field. Under other disadvantageous conditions there may appear additional sets of fringes. The design role of the aperture stop in the interferometer is to eliminate the useless reflected light beams mentioned above. For this reason the diameter of the aperture stop ought to be small enough to transmit solely the beams generating the proper fringe pattern.

---

* The problem was signalled by R. Jóźwicki and W. Sawicki at the VIII Polish-Czechoslovakian Optical Conference, Szklarska Poręba, September 13–16, 1988

The wavefront falling on the standard and measured elements is defined in a finite area only because of the finite element dimensions. Therefore the intensity distribution in the aperture stop plane has the form of the diffraction image of two points, where one of the point images is generated by the light reflected from the measured surface and the second one — from the standard surface. Theoretically, the field distribution in the diffraction image is spread all over an infinitely large area. Therefore it must be truncated by the aperture stop. The problem is to estimate the influence of this truncation upon the intensity distribution in the observation field of an interferometer.

## 2. General considerations

Let our problem be considered on the basis of Fizeau interferometer shown in Fig. 1. For simplicity the flatness measurement will be analysed. A point source *SR* emitting the monochromatic light of wavelength $\lambda$ is set at the object focus of the objective *U*. If we assume that the objective *U* is free of aberrations, then the plane wave will be observed in the image space of *U*. The interferometer is applied to measure the shape of the surface *b* of a tested element *T* by comparing it with the surface *c* of a standard *S*. Theoretically both surfaces should be planar. The plane wave after reflection from the surfaces *b* and *c* generates two waves which, after transmission through the objective *U* and the reflection from the beam splitter *B*, focus inside the aperture stop *AS*. The wave falling on the standard and the tested element generates also the useless wavefronts reflected from the surfaces *d* and *e* of these elements. The aperture stop has to stop these beams. This is possible if the surfaces *c* and *e* of the standard and also the surfaces *b* and *d* of the tested element are not pairwise parallel, which usually takes place in practice. The fringe image is registered in the plane of a detector *D*. The imaging system $U_i$ is telecentric on the detector side to avoid the measurement error. The detector plane coincides with the image of the surface *b* of

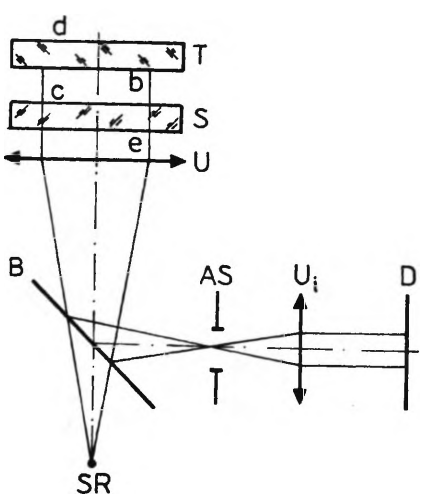


Fig. 1. Optical system of Fizeau interferometer for the flatness measurement

the element under test, given by the combined optical system $U + U_i$. The objective $U$, the standard $S$ and the tested element $T$ have finite dimensions. Therefore the waves reflected from $T$ and $S$ are defined in the finite area, and in the aperture stop plane one sees the diffraction image in the form of two spot images. The truncation of this image by the aperture stop may influence the fringe pattern monitored on the detector plane $D$.

To simplify our study the analyses can be transferred into the space between the objectives $U$ and $U_i$, and in this case the interferometric system shown in Fig. 1 can be reduced to systems shown in Fig. 2.

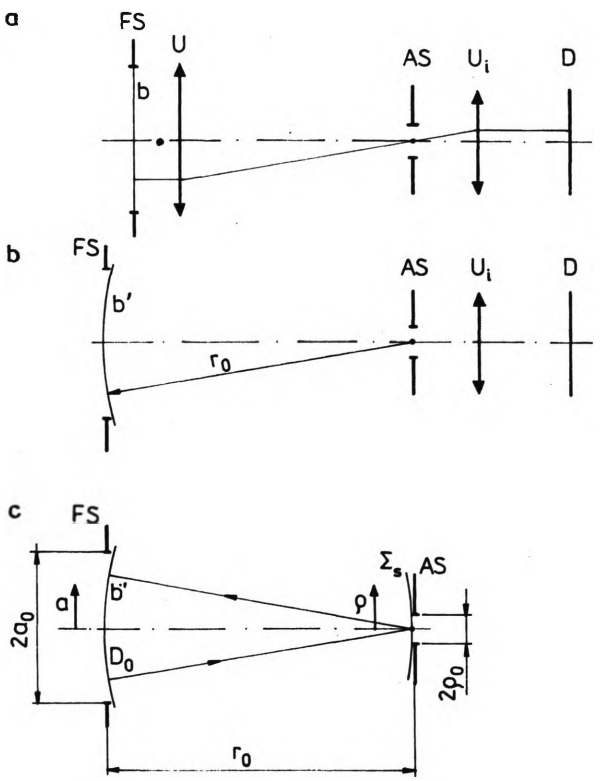


Fig. 2. Evolvement of the optical system of Fig. 1 into the substitutional systems. The reflecting planes (**a**), the objective $U$ (**b**), and the objective $U_i$ (**c**) have been neglected

At first we can evolve the imaging system neglecting the beam splitter (see Fig. 2**a**). We shall consider only the wave reflected from the surface $b$ of the element under test, because the wave reflected from the surface $c$ of the standard behaves exactly like the wave under consideration. Moreover, the fragment of the optical system forming the wave falling onto the tested element, being unessential from the view point of our analysis, has been neglected. Additionally, a field stop $FS$ in the plane $b$ has been set, assuming the beam truncation by the tested element. This means that

the diameter of the objective $U$ is assumed to be appropriately larger than the diameter of $FS$.

If the objective $U$ is aberration-free, then according to the synthesis of the optical system [3] the objective can be neglected in the further analysis. It is sufficient to consider only the image $b'$ of the plane $b$ given by this objective (see Fig. 2**b**). Besides the fact that the image field distribution on $b'$ differs in scale from the boject field distribution on $b$ (which refers to the magnification of the objective $U$ for the plane $b$) it is defined on the sphere (not on the plane) according to the principle of the reference sphere transformation [4]. For the known object field distribution in the plane $b$ (the spherical surface with centre at infinity), the centre of the image sphere $b'$ is at the image focus of the objective $U$, which coincides with the aperture stop plane $AS$ (see Fig. 2**a**).

The operation used for the objective $U$ can be repeated for the objective $U_i$, hence the optical system from Fig. 2**b** can be reduced to the system shown in Fig. 2**c**. The detector plane $D$ being optically conjugate with the plane $b$ by the combined system $U + U_i$ (Fig. 2**a**), the plane $D$ must be also conjugate with the sphere $b'$ by the system $U_i$ (Fig. 2**b**). This fact can be also proved with the aid of the principle of the reference sphere transformation.

After the plane $D$ is transferred through the objective $U_i$ to its object space, the following stages of the wave propagation in the interferometric optical system can be considered (see Fig. 2**c**):

1. Generation of a field distribution on the sphere $\Sigma_s$ by a field distribution from the sphere $b'$; this stage corresponds to the wave propagation from the plane $b$ to the aperture stop plane $AS$ in Fig. 2**a**. This operation can be performed by the Fourier transformation. The field distribution on the sphere $\Sigma_s$ is the Fourier spectrum of the field distribution from the sphere $b'$.

2. Truncation of the Fourier spectrum on the sphere $\Sigma_s$ by the aperture stop $AS$ (transmission through the aperture stop $AS$ in Fig. 2**a**).

3. Generation of a field distribution on the detector sphere $D_0$ by the truncated Fourier spectrum from the sphere $\Sigma_s$ (the wave propagation from the aperture stop plane $AS$ to the plane $D$ in Fig. 2**a**). The operation is performed by the inverse Fourier transformation.

It is worth to ephasize that in Fig. 2**c** the spheres $b'$ and $D_0$ coincide but actually they refer to the different elements in the real system shown in Fig. 1 (or in Fig. 2**a**).

From the view point of the phenomenon analysis the system shown in Fig. 2**c** is fully equivalent to the real system, but by neglecting the objectives $U$ and $U_i$ the analyses are essentially simplified. For clarity the successive stages of the consideration are marked in the figure by arrows.

## 3. Analysis

We will consider the problem for systems with rotational symmetry when instead of the Fourier transformation the Hankel one can be used. It means that the plane $b$ in

Fig. 2a is perpendicular to the optical axis and the centre of the point image coincides with the centre of the aperture stop *AS*. A more general case [6] with a tilt of the plane *b* (eccentric position of the point image in the aperture stop) can be also considered, but the most significant intensity changes in the observation field occur in the case taken for consideration (see conclusions in Sec. 6).

Let $V(a)$ be the field distribution on the sphere $b'$ (Fig. 2c). The field distribution $V_s(\varrho)$ on the sphere $\Sigma_s$ corresponding to the Fourier spectrum of the field $V(a)$ can be found from the following relation [5]

$$V_s(\varrho) = \frac{2\pi}{\lambda r_0} \int_0^{a_0} V(a)\, J_0\left(\frac{ka\varrho}{r_0}\right) a\,da \tag{1}$$

where $a$, $\varrho$ are radial coordinates defining the positions of points on the spheres $b'$ and $\Sigma_s$, respectively, $r_0$ – distance between the spheres $b'$ and $\Sigma_s$, $2a_0$ – diameter of the field stop *FS*, $k = 2\pi/\lambda$, $J_0(x)$ – zero order Bessel function of an argument $x$. All dimensions are related to the space of the substitutional system, Fig. 2c.

If the diameter of the aperture stop *AS* is denoted by $2\varrho_0$, then the field distribution on the sphere $D_0$, after the truncation of the Fourier spectrum by the aperture stop, is described by the equation

$$V'(a) = \frac{2\pi}{\lambda r_0} \int_0^{\varrho_0} V_s(\varrho)\, J_0\left(\frac{ka\varrho}{r_0}\right) \varrho\, d\varrho. \tag{2}$$

In the case shown in Fig. 1 for the system *U* free of aberrations there is a constant complex amplitude distribution on the plane *b*. Consequently, the constant complex amplitude distribution occurs also on the sphere $b'$ inside the field stop *FS* (Fig. 2c) ($V(a) = V_0$ in Eq. (1)). According to [1] the well known expression describing the field distribution on the sphere $\Sigma_s$ is obtained as

$$V_s(Z) = \frac{\pi a_0^2 V_0}{\lambda r_0} \frac{2J_1(Z)}{Z} \tag{3}$$

where

$$Z = \frac{ka_0\varrho}{r_0} \tag{4}$$

is the parametrized radial coordinate $\varrho$, $J_1(x)$ is the first order Bessel function of an argument $x$. The field described by Eq. (3) is known as the Airy pattern [1], see Sec. 8.5.2. This is the Fourier spectrum of the uniform field defined in the circular area.

After substitution of Equation (3) into (2) it will be

$$V'(a_n) = V_0 \int_0^{Z_0} J_1(Z)\, J_0(a_n Z)\, dZ \tag{5}$$

where

$$a_n = a/a_0 \tag{6}$$

is the normalized radial coordinate $a$, and $Z_0 = Z$ for $\varrho = \varrho_0$. The quantity $Z_0$ is a measure of the truncation degree. The intensity distribution can be found from the expression

$$I'(a_n) = [V'(a_n)]^2 \tag{7}$$

because $V'(a_n)$ is real.

The demanded relations (5) and (7) allow us to find the intensity distribution in the observation field of an interferometer, when the truncation by the aperture stop is taken into account. The distribution concerns one of the interfering waves reflected from the standard surface or from the tested element surface. For the substitutional system of Fig. 2c the image intensity distribution is defined on the sphere $D_0$. For the real system the distribution under consideration arises on the detector plane $D$ (Fig. 1). The edge of the image field occurs at $a_n = 1$.

Theoretically, in the area of the observation field the field distribution ought to be constant. This is true if $Z_0 \to \infty$ (the case without truncation by the aperture stop) because, according to (5), (7) and [7] (formula number 6.512.3), we have $I'(a_n = I_0 = V_0^2$ for $a_n < 1$ and $I'(a_n) = 0$ for $a_n > 1$. For finite value of $Z_0$ the function $I'(a_n)$, according to (5) and (7), can be determined by a numerical method. The analytical solution of Eq. (5) exists in the two following cases:

i) for $a_n = 0$, because $J_0(0) = 1$, and according to formula 6.511.7 in [7]

$$I'(0) = I_0[1 - J_0(Z_0)]^2, \tag{8}$$

ii) for $a_n = 1$, according to formula 6.512.7 in [7] and formula (83) in [8], after rearrangement we get

$$I'(1) = 0.25\, I_0[1 - J_0^2(Z_0)]^2. \tag{9}$$

## 4. Results

In order to characterize the phenomenon we will present some intensity distributions $I'(a_n)$ obtained by numerical methods for different truncation degrees $Z_0$. To this end, as it was mentioned, we may use the integral (5). Because of the oscillatory character of Bessel functions, the computer standard procedures are not convenient for large values of the truncation degree $Z_0$. We have applied our own procedure using the sampling theorem for Fourier and Hankel transformations. The method has been proposed by SZAPIEL in [9]. The relations (8) and (9) derived on account of the integral (5) have facilitated only, the verification of our calculations. The procedure used is general, this means that it may be applied to different field distributions. Using this procedure step by step two times, first to calculate the field distribution on the sphere $\Sigma_s$ (Fig. 2c), and next to find the field on the sphere $D_0$, it is possible to estimate the influence of the beam truncation by the aperture stop in the case of aberrated optical system or in the nonuniform illumination. As an example we will present the results obtained for the truncated Gaussian beam, this case being typical of an interferometer illuminated by a laser.

In order to facilitate the application of the results obtained it is advisable to express the truncation degree $Z_0$ by the Airy number $A$, for which

$$Z_0 = x_1 A \tag{10}$$

where $x_1$ is the first root of Bessel function $J_1(x)$ ($x_1 = 3.8317\ldots$). The diameter of the first dark ring of the Airy pattern equals $2x_1$, this means that the Airy number indicates how many times the aperture stop diameter is larger than the diameter of the central part of the Airy pattern (see Fig. 3). In the cases without uniform field, when the point image has not the form of Airy pattern, the quantity $A$ can also be used conveniently as a reference measure with respect to the uniform field case.

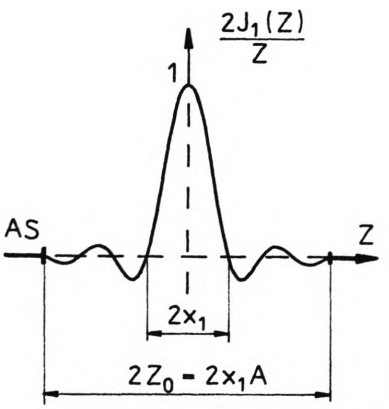


Fig. 3. Definition of the Airy number $A$

In Figures 4–7 the cases with the uniform field are shown for different values of $A$. Because of rotational symmetry the distributions are presented only in the half sections. The theoretical case without truncation ($A \to \infty$) is marked with a dashed line. For simplicity the normalized distribution has been taken as

$$I'_n(a_n) = I'(a_n)/I_0. \tag{11}$$

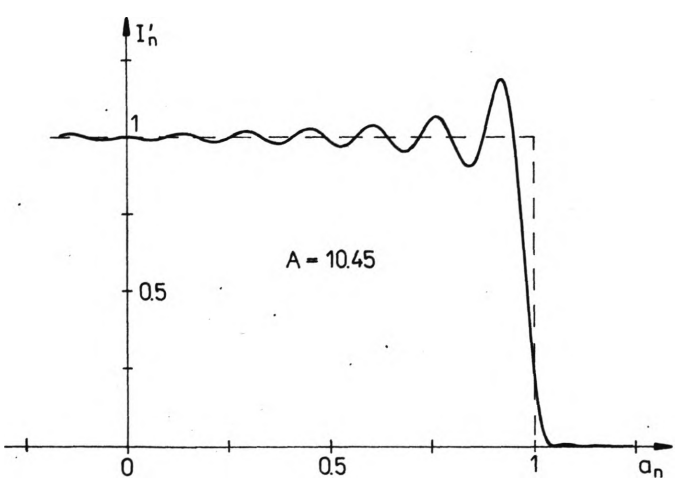


Fig. 4. Intensity distribution in the observation field for $A = 10$ (uniform illumination)

In the case without truncation the intensity distribution $I'(a_n)$ equals $I_0$ and the normalized intensity distribution $I'_n(a_n) = 1$ for $a_n < 1$.

Based on Figures 4 and 5, given for Airy numbers $A = 10$ and $A = 30$, respectively, we can conclude that in the meridional sections the field truncation by the aperture stop introduces the oscillatory changes of the intensity distributions. The change of the mean value of the intensity is of no importance, because the field truncated by the aperture stop is small if compared to the field of the central part of the Airy pattern. With the increasing $A$ the period $t_a$ (Fig. 3) of the oscillatory changes of the intensity decreases. It can be shown that [6]

$$t_a A \approx 1.6. \tag{12}$$

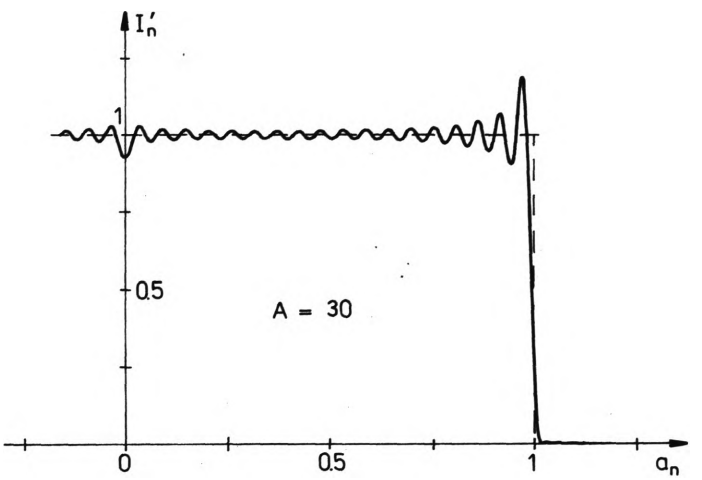


Fig. 5. Intensity distribution in the observation field for $A = 30$ (uniform illumination)

In general, with the increasing $A$ the amplitude of the intensity changes decreases, but this phenomenon is more complex in details. The axial value of the intensity is described by Eq. (8). The function $J_0(x)$ can take the negative as well as positive values, i.e., $I'_n(0) > 1$ or $I'_n(0) < 1$, respectively. From the asymptotic expansion of $J_0(x_1 A)$ valid for $x_1 A \gg 0$ (see formula 18 of [8]) we have

$$J_0(x_1 A) \cong \sqrt{\frac{2}{\pi x_1 A}} \cos(x_1 A - \pi/4). \tag{13}$$

The maximum and minimum values of $J_0(x_1 A)$ for $A$ close to 10 occur at $A = 10.86$ and $A = 10.04$, respectively. The intensity distributions in these cases are shown in Fig. 6. The oscillatory changes of the axial intensity are connected with the phase jump by $\pi$ of the field distribution on crossing each dark ring of the Airy pattern (see Fig. 3). With the increase of $A$ the amplitude of the axial changes slowly decreases, what results from Eq. (13). For $A = 10.45$ we have $J_0(x_1 A) = 0$ and, according to (8) and (11), $I'_n(0) = 1$, see Fig. 7. Comparing Figures 6 and 7 we can conclude that the

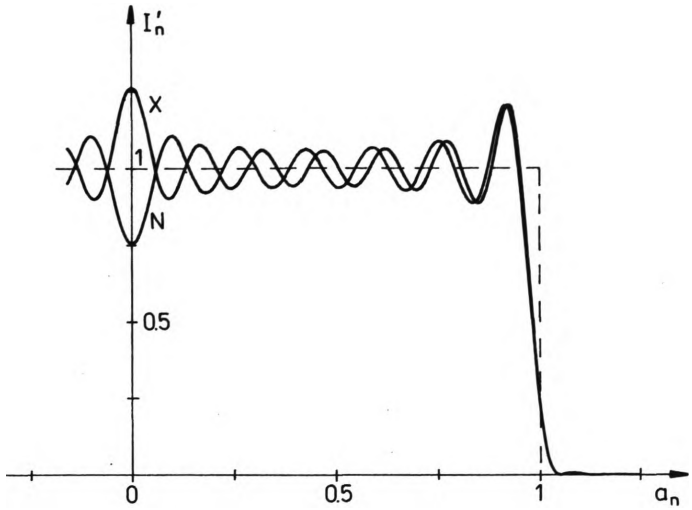


Fig. 6. Intensity distributions in the observation field with a minimum axial intensity ($N$) for $A = 10.04$, and with the maximum axial intensity ($X$) for $A = 10.86$ (uniform illumination)

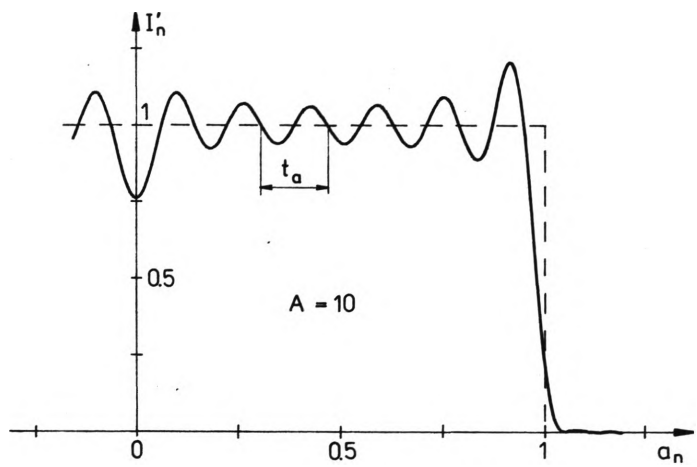


Fig. 7. Intensity distribution in the observation field with the axial intensity $I'_n = 1$ for $A = 10.45$ (uniform illumination)

oscillations of the intensity distributions in the whole meridional section occur in the cases of the minimum or maximum axial intensity. If the axial intensity $I'_n(0) = 1$, then the intensity oscillations in the axial area almost disappear, but they increase with the increasing radial distance $a_n$. At the edge of the observation field there occurs the Gibbs phenomenon [10] and the value of the intensity at the edge maximum does not depend on the Airy unit ($I'_n \approx 1.19$). The width of the edge maximum is nearly equal to one half of the period ($0.5\,t_a$). This means that it decreases with the increasing Airy number $A$ according to Eq. (12). The oscillations

of the intensity distribution outside the observation field ($a_n > 1$) for $A \geqslant 10$ are negligibly small.

Figure 8 shows the case of the Gaussian apodisation, when the diameter of the observation field is two times smaller than the diameter of the Gaussian distribution. Comparing Figs. 5 and 8 we can conclude that the intensity distribution changes are

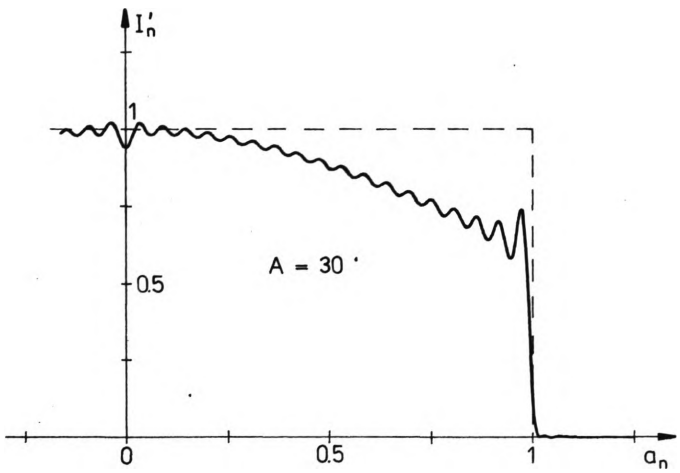


Fig. 8. Intensity distribution in the observation field for $A = 30$ (Gaussian apodisation)

in both cases (without apodisation and with Gaussian apodisation) of a similar character. The intensity changes in the case of Gaussian apodisation are slightly smaller, in particular at the edge of the observation field.

## 5. Experimental verification

The experiment has been performed with the system shown in Fig. 9. The wavefront generated by a laser $L$ is focused by the microscopic objective $O_1$ in the pinhole plane $P$. The beam divergence in the image space of $O_1$ is so large that the wave falling on the objective $O_2$ can be considered as a spherical one. A convergent spherical wave propagating with the centre in the plane of the aperture stop $AS$ propagates in the image space of $O_2$. The image of the field stop $FS$, given by the objective $O_3$, is registered in the plane $D$. The photograph of the observation field for $A \approx 3.5$ is given in Fig. 10. The value of $A$ refers to the fourth dark ring of the Airy pattern (the

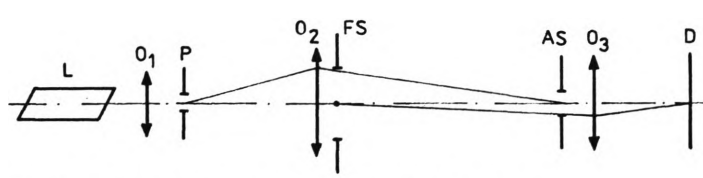


Fig. 9. Optical system for experimental verification

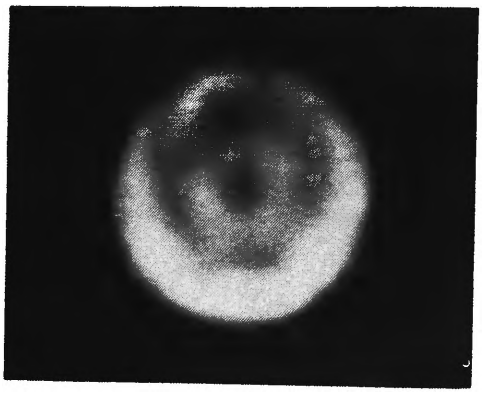

Fig. 10. Photograph of the observation field for $A \approx 3.5$ (uniform illumination)

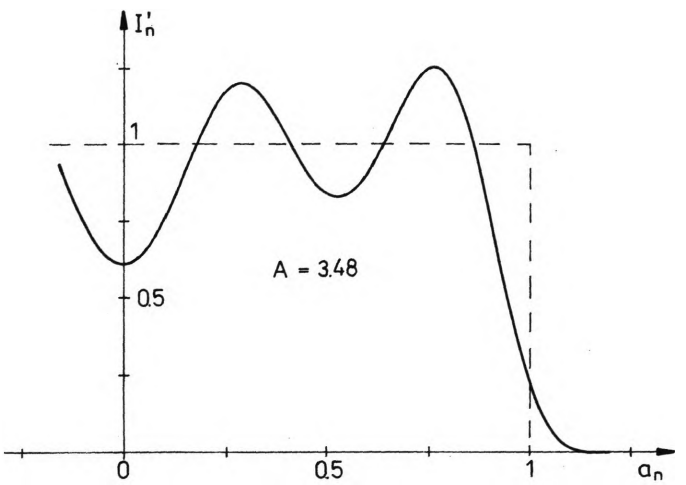


Fig. 11. Intensity distribution in the observation field for $A = 3.48$ (uniform illumination)

case shown in Fig. 3) and, simultaneously, to the minimum axial intensity. The calculated intensity distribution for this case is presented in Fig. 11. Taking into account the speckle noise of the laser illumination we can admit that the experimental and analytical results are in agreement.

## 6. Practical conclusions

The aperture stop of the interferometers influences the intensity distribution in the observation field. In practice, however, if the quotient of diameters of the aperture stop and the Airy first ring (the number $A$) is large (for example, larger than 30), the intensity changes are not essential (see Fig. 5, for conclusion). In an interferometer with the field observation diameter $2a_0 = 200$ mm, the focal length of the objective $U$ (Fig. 1) is equal to 1000 mm, the wavelength $\lambda = 0.633$ μm, and the diameter of

the first dark ring is equal to

$$2\varrho_1 = \frac{2x_1 f'}{ka_0} = \frac{1.22\lambda f'}{a_0} = 3.86 \ \mu\text{m}.$$

For the diameter of the aperture stop $2\varrho_0 = 0.5$ mm we have $A = 130$. As this diameter may be also larger, the influence of the aperture stop can be considered as being negligibly small. Moreover, some eccentricity of the Airy pattern with respect to the centre of the aperture stop [6], or some irregularity of the stop edge, decreases the intensity changes in the central part of the observation field (like in Fig. 7). This is because some field rings of the Airy pattern lying near the stop edge are truncated partially. A combination of the fields with the phases 0 and $\pi$ decreases the intensity oscillations. This phenomenon related to the eccentric displacement of the aperture stop $AS$ was observed in the experiment described in Section 5.

The influence of the Fourier spectrum truncation upon the intensity distribution in the observation field may be essential in the multipass interferometry [11]. In this case, to improve the measurement accuracy, the wave passes several times through a tested element. The choice of the pass number is achieved by a proper filtering of the Fourier spectrum, which is connected with its strong truncation.

## References

[1] BORN M., WOLF E., *Principles of Optics*, Pergamon Press, Oxford 1980, see, for example, Chapt. VII.
[2] RODIONOV S. A., AGUROK I. P., Opt. Mech. Prom., No. 6 (1971), 63 (in Russian).
[3] JÓŹWICKI R., Opt. Acta **31** (1984), 169.
[4] JÓŹWICKI R., Opt. Acta **29** (1982), 1383.
[5] JÓŹWICKI R., *Theory of Optical Imaging*, [Ed.] PWN, Warszawa 1988, p. 90 (in Polish).
[6] SAWICKI W., Master Thesis, Warsaw University of Technology, 1988 (in Polish).
[7] GRADSHTEYN I. S., RYZHIK I. M., *Table of Integrals, Series and Products*, Academic Press, New York 1980.
[8] MCLACHLAN N. W., *Bessel Functions for Engineers*, Clarendon Press, Oxford 1955 (see List of the Formulae).
[9] SZAPIEL S., J. Opt. Soc. Am. **A4** (1987), 4.
[10] CHAMPENEY D. C., *Fourier Transforms and their Physical Applications*, Academic Press, London 1973, p. 6.
[11] LANGENBECK P. H., Appl. Opt. **8** (1969), 543.

*Received May 4, 1989*

## Влияние ограничения поля апертурной диафрагмой интерферометров на распределение напряжения в поле зрения

Теоретически испытано влияние сужения введенного апертурной диафрагмой в интерферометрических системах. Рассмотрены случаи с однородным освещением и гауссовской аподизацией. Обнаружено возникновение осцилляционных изменений интенсивности в поле зрения, но в большинстве практических случаев они незаметно малы. Это явление можно считать существенным в случае интерферометрии многократного прохода, когда применяется сильное сужение. Представили экспериментальную проверку.